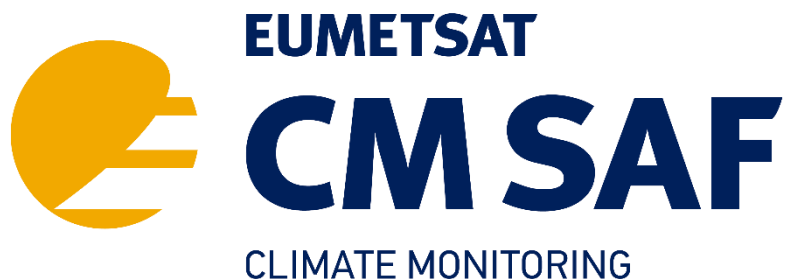


EUMETSAT Satellite Application Facility on Climate Monitoring



Validation Report

Microwave Imager Radiance FCDR

SSM/I Brightness Temperatures

DOI: 10.5676/EUM_SAF_CM/FCDR_MWI/V004

Microwave Imager Radiance FCDR R4

CM-12003

Reference Number:


SAF/CM/DWD/VAL/FCDR_SSMI

Issue/Revision Index:

1.2

Date:

2022-01-31

	Validation Report Microwave Imager Radiance FCDR R4 SSM/I Brightness Temperatures	Doc. No: SAF/CM/DWD/VAL/FCDR_SSMI Issue: 1.2 Date: 2022-01-31
---	--	---

Document Signature Table

	Name	Function	Signature	Date
Author	Karsten Fennig	CM SAF scientist		2022-01-31
Editor	Marc Schröder	Science Coordinator		2022-01-31
Approval	CM SAF Steering Group			
Release	Rainer Hollmann	Project Manager		


Distribution List

Internal Distribution	
Name	No. Copies
DWD / Archive	1
CM SAF Team	1

External Distribution		
Company	Name	No. Copies
PUBLIC		1

Document Change Record

Issue/ Revision	Date	DCN No.	Changed Pages/Paragraphs
0.9	2012-10-29	SAF/CM/DWD/VAL/FCDR_SSMI/0.9	Version for review.
1.0	2013-01-31	SAF/CM/DWD/VAL/FCDR_SSMI/1.0	Changes following review.
1.1	2017-01-18	SAF/CM/DWD/VAL/FCDR_SSMI/1.1	Update DOI for FCDR MWI R3
1.2	2022-01-31	SAF/CM/DWD/VAL/FCDR_SSMI/1.2	Update for DRR 3.1

	Validation Report Microwave Imager Radiance FCDR R4 SSM/I Brightness Temperatures	Doc. No: SAF/CM/DWD/VAL/FCDR_SSMI Issue: 1.2 Date: 2022-01-31
---	--	---

Applicable documents

Reference	Title	Code / Validity Date
AD 1	Memorandum of Understanding between CM SAF and the Max-Planck Institute for Meteorology and Meteorological Institute, University of Hamburg	1. March 2012
AD 2	CM SAF Product Requirements Document	SAF/CM/DWD/PRD/2.0

Reference documents

Reference	Title	Code
RD 1	Product User Manual Fundamental Climate Data Record of SSM/I Brightness Temperatures	SAF/CM/DWD/PUM/ FCDR_SSMI/1.2
RD 2	Algorithm Theoretical Basis Document Fundamental Climate Data Record of SSM/I Brightness Temperatures	SAF/CM/DWD/ATBD/ FCDR_SSMI/2.2
RD 3	Validation Report Fundamental Climate Data Record of SMMR / SSM/I / SSMIS Brightness Temperatures	SAF/CM/DWD/VAL/ FCDR_MWI/1.4

Table of Contents

Preface.....	7
1 The EUMETSAT SAF on Climate Monitoring.....	7
2 Introduction	8
3 Instrument and sensor stability	9
4 Evaluation of Brightness Temperature differences.....	12
4.1 Data Sets for Comparison.....	13
4.2 Visual inspection	13
4.3 Evaluation strategy.....	15
4.4 Evaluation Results.....	17
5 Conclusions.....	33
6 References.....	34
7 Glossary.....	34

List of Tables

Table 2-1: FCDR instrument data availability.....	9
Table 4-1: Requirements for SSM/I brightness temperatures product as given in the PRD [AD 2].	16
Table 4-2: Statistics of the ensemble anomalies for SSM/I channel 19v GHz. The first block shows the original RDR with EIA normalized, the second block the CM SAF FCDR and the last block the RSS V6 FCDR. The offsets depict the differences between CM SAF and RSS over ocean.....	20
Table 4-3: Statistics of the ensemble anomalies for SSM/I channel 19h GHz. The first block shows the original RDR with EIA normalized, the second block the CM SAF FCDR and the last block the RSS V6 FCDR. The offsets depict the differences between CM SAF and RSS over ocean.....	22
Table 4-4: Statistics of the ensemble anomalies for SSM/I channel 22v GHz. The first block shows the original RDR with EIA normalized, the second block the CM SAF FCDR and the last block the RSS V6 FCDR. The offsets depict the differences between CM SAF and RSS over ocean.....	24
Table 4-5: Statistics of the ensemble anomalies for SSM/I channel 37v GHz. The first block shows the original RDR with EIA normalized, the second block the CM SAF FCDR and the last block the RSS V6 FCDR. The offsets depict the differences between CM SAF and RSS over ocean.....	26
Table 4-6: Statistics of the ensemble anomalies for SSM/I channel 37h GHz. The first block shows the original RDR with EIA normalized, the second block the CM SAF FCDR and the last block the RSS V6 FCDR. The offsets depict the differences between CM SAF and RSS over ocean.....	28
Table 4-7: Statistics of the ensemble anomalies for SSM/I channel 85v GHz. The first block shows the original RDR with EIA normalized, the second block the CM SAF FCDR and the last block the RSS V6 FCDR. The offsets depict the differences between CM SAF and RSS over ocean.....	30


	Validation Report Microwave Imager Radiance FCDR R4 SSM/I Brightness Temperatures	Doc. No: SAF/CM/DWD/VAL/FCDR_SSM/I Issue: 1.2 Date: 2022-01-31
---	--	--

Table 4-8: Statistics of the ensemble anomalies for SSM/I channel 85h GHz. The first block shows the original RDR with EIA normalized, the second block the CM SAF FCDR and the last block the RSS V6 FCDR. The offsets depict the differences between CM SAF and RSS over ocean..... 32

List of Figures

Figure 3-1: Time series of DMSP platform mean local equator crossing times, altitude and the Earth Incidence Angles of the different SSM/I instruments. Thin lines are the mean values at the ascending equator crossing and thick lines depict complete orbit mean values. Colours are as follows: F08 orange, F10 blue, F11 black, F13 green, F14 violet, and F15 red. 10

Figure 3-2: Time series of SSM/I sensor diagnostics: Temperature of the warm calibration target (upper panel) and radiometer sensitivities for the channels at 19v, 19h, and 22v GHz (centre and lower panel). The grey lines denote 0°C for the hot load temperature and the specification values for the radiometer sensitivities; for colours see Figure 3-1. 11

Figure 4-1: Time series of SSM/I sensor diagnostics: Radiometer sensitivities for the channels at 37v, 37h, 85v and 85h GHz. The grey lines denote the specification values; for colours see Figure 3-1.... 12

Figure 4-2: Climatological mean of SSM/I TB differences at 19 GHz between F13 and F15. In the left column shows the original uncorrected raw data records. The middle column depicts the CM SAF FCDR and the right column shows the RSS FCDR. The top row shows the vertical polarisation, the middle row the horizontal polarisation and in the bottom row depicts the double differences between both polarisations..... 14

Figure 4-3: As Figure 4-2 but for the SSM/I TB differences at 19 GHz between F11 and F10. 15

Figure 4-4: Time series of ensemble anomalies and variability for SSM/I channel 19v GHz. In the upper two panels the solid lines are PM orbits and the dashed lines AM orbits. The lower panels depict daily means of AM and PM orbits. The grey lines depict the ensemble spread. Horizontal dotted grey lines denote the optimal bias and the target RMS value (lowest panel). For a detailed description see text (section 4.3). 19

Figure 4-5: Same as Figure 4-4, but for SSM/I channel 19h GHz. 21


Figure 4-6: Same as Figure 4-4, but for SSM/I channel 22v GHz. 23

Figure 4-7: Same as Figure 4-4, but for SSM/I channel 37v GHz. 25

Figure 4-8: Same as Figure 4-4, but for SSM/I channel 37h GHz. 27

Figure 4-9: Same as Figure 4-4, but for SSM/I channel 85v GHz. 29

Figure 4-10: Same as Figure 4-4, but for SSM/I channel 85h GHz. 31

	Validation Report Microwave Imager Radiance FCDR R4 SSM/I Brightness Temperatures	Doc. No: SAF/CM/DWD/VAL/FCDR_SSMI Issue: 1.2 Date: 2022-01-31
---	--	---

Preface

This document is structured in two different logical parts, reflecting the different instrument series used to compile a Fundamental Climate Data Record (FCDR) from conical scanning microwave imagers. After a short introduction, summarizing the current status, this document focuses on the validation of the Special Sensor Microwave / Imager (SSM/I) component of the FCDR. This part is unchanged since the first release of this FCDR ([DOI:10.5676/EUM_SAF_CM/FCDR_SSMI/V001](https://doi.org/10.5676/EUM_SAF_CM/FCDR_SSMI/V001)). The corresponding document for the parts from the Scanning Multichannel Microwave Radiometer (SMMR) and the Special Sensor Microwave Imager/Sounder (SSMIS) are referenced here [RD 3].


1 The EUMETSAT SAF on Climate Monitoring

The importance of climate monitoring with satellites was recognized in 2000 by EUMETSAT Member States when they amended the EUMETSAT Convention to affirm that the EUMETSAT mandate is also to “contribute to the operational monitoring of the climate and the detection of global climatic changes”. Following this, EUMETSAT established within its Satellite Application Facility (SAF) network a dedicated centre, the SAF on Climate Monitoring (CM SAF, <http://www.cmsaf.eu/>).

The consortium of CM SAF currently comprises the Deutscher Wetterdienst (DWD) as host institute, and the partners from the Royal Meteorological Institute of Belgium (RMIB), the Finnish Meteorological Institute (FMI), the Royal Meteorological Institute of the Netherlands (KNMI), the Swedish Meteorological and Hydrological Institute (SMHI), the Meteorological Service of Switzerland (MeteoSwiss), the Meteorological Service of the United Kingdom (UK MetOffice) and the Centre National de la Recherche Scientifique, Laboratoire d’études en Géophysique et Océanographie Spatiales, France (CNRS, LEGOS). Since the beginning in 1999, the EUMETSAT Satellite Application Facility on Climate Monitoring (CM SAF) has developed and will continue to develop capabilities for a sustained generation and provision of Climate Data Records (CDR’s) derived from operational meteorological satellites.

In particular the generation of long-term data sets is pursued. The ultimate aim is to make the resulting data sets suitable for the analysis of climate variability and potentially the detection of climate trends. CM SAF works in close collaboration with the EUMETSAT Central Facility and liaises with other satellite operators to advance the availability, quality and usability of Fundamental Climate Data Records (FCDRs) as defined by the Global Climate Observing System (GCOS). As a major task the CM SAF utilizes FCDRs to produce records of Essential Climate Variables (ECVs) as defined by GCOS. Thematically, the focus of CM SAF is on ECVs associated with the global energy and water cycle.

The CM SAF data sets can serve applications related to the new Global Framework of Climate Services initiated by the WMO World Climate Conference-3 in 2009. CM SAF is supporting climate services at national meteorological and hydrological services (NMHSs) with long-term data records but also with data sets produced close to real time that can be used to prepare monthly/annual updates of the state of the climate. Both types of products together allow for a consistent description of mean values, anomalies, variability, and potential trends for the chosen ECVs. CM SAF ECV data sets also serve the improvement of climate models both at global and regional scale.

	Validation Report Microwave Imager Radiance FCDR R4 SSM/I Brightness Temperatures	Doc. No: SAF/CM/DWD/VAL/FCDR_SSMI Issue: 1.2 Date: 2022-01-31
---	--	---

A catalogue of all available CM SAF products is accessible via the CM SAF webpage, <http://www.cmsaf.eu/>. Here, detailed information about product ordering, add-on tools, sample programs and documentation is provided.

2 Introduction


This CM SAF validation report provides information on the evaluation of the CM SAF Fundamental Climate Data Record (FCDR) of Microwave Brightness Temperatures from the conical scanning microwave sensors Special Sensor Microwave/Imager (SSM/I), Special Sensor Microwave Imager/Sounder (SSMIS) and Scanning Multichannel Microwave Radiometer (SMMR). This fourth release is a continuation of the previous release (available from CM SAF; http://dx.doi.org/10.5676/EUM_SAF_CM/FCDR_MWI/V003).

Data from the space-borne microwave imagers and sounders such as the Scanning Multichannel Microwave Radiometer (SMMR), Special Sensor Microwave/Imager (SSM/I) and the Special Sensor Microwave Imager/Sounder (SSMIS) are used for a variety of applications, such as analyses of the hydrological cycle (precipitation and evaporation) and related atmospheric and surface parameters, as well as remote sensing of sea ice, soil moisture, and land surface temperatures. Carefully calibrated and homogenised radiance data sets are a fundamental prerequisite for climate analysis, climate monitoring and reanalysis. Several National Meteorological Services and Reanalysis centres assimilate microwave radiances directly and not derived geophysical parameters. Forecast and reanalysis can thus benefit from a Fundamental Climate Data Record (FCDR) of brightness temperatures (Poli et al. 2015). The generation of Thematic Climate Data Records (TCDRs) strongly relies on the availability of FCDRs. Highest possible TCDR quality can be achieved easiest in radiance space, in turn increasing the products value for users.

The predecessors of this data record and the data processor suite have originally been developed at the Max-Planck Institute for Meteorology (MPI-M) and the University of Hamburg (UHH) for the Hamburg Ocean Atmosphere Parameters and Fluxes from Satellite Data (HOAPS, <http://www.hoaps.org/>) climatology. HOAPS is a compilation of climate data records for analysing the water cycle components over the global oceans derived from satellite observation (Andersson et al. 2011). The main satellite instrument employed to retrieve the geophysical parameters is the SSM/I and much work has been invested to process and carefully homogenize all SSM/I instruments on-board the Defence Meteorological Satellite Program (DMSP) platforms F08, F10, F11, F13, F14 and F15 (Andersson et al., 2010).

The HOAPS processing suite has been transferred to CM SAF in a Research to Operations activity in order to provide a sustained processing of the climate data records which is one of the main tasks of CM SAF, but not in the focus of the research group at the MPI-M / UHH. The operational processing and reprocessing of the FCDRs and TCDRs as well as the provision to the research community is maintained and coordinated by the CM SAF.

The first release of the CM SAF FCDR (Fennig et al. 2013) focussed on the SSM/I series, covering the time period from 1987 to end of 2008. In order to continue the HOAPS TCDRs beyond 2008 it was necessary to extend the underlying FCDR of microwave TBs with the SSMIS sensor family aboard the DMSP platforms F16, F17, and F18, which was accomplished with the second release of the CM SAF FCDR (Fennig et al. 2015). This combined FCDR of SSM/I and SSMIS brightness temperatures provides a consistent FCDR from 1987 to 2013.

	Validation Report Microwave Imager Radiance FCDR R4 SSM/I Brightness Temperatures	Doc. No: SAF/CM/DWD/VAL/FCDR_SSMI Issue: 1.2 Date: 2022-01-31
---	--	---

Following requests from users of the FCDR, the third release focussed on the extension of the microwave brightness temperature data record to the earlier time period from 1978 to 1987 with observations from the SMMR on-board Nimbus 7 and the extension of the SSMIS period to 2015. However, it turned out to be a very challenging task, as it has not been possible to get hold of the original raw instrument data records. Although this data record must have eventually been transferred from the Marshall Space Flight Centre (MSFC) to the National Snow & Ice Data Center (NSIDC), it is currently not available from their archives. Instead, the Nimbus-7 SMMR Pathfinder Level 1B Brightness Temperatures data record, available from NSIDC (Njoku, 2003), was used to generate this FCDR.

The third release of the FCDR is described in Fennig et al. (2020) which also includes a decent overview of the applied methodologies.

With the fourth release of the Microwave Imager Radiance FCDR, the temporal coverage of the SSMIS has been extended to 31 December 2020 while the SMMR and SSM/I data records remain unchanged.

A technical description of the data sets including information on the file format as well as on the data access is provided in the Product User Manual [RD 1]. Furthermore details on the CM SAF inter-sensor calibration model, the implementation of the processing chain and individual processing steps are available in the Algorithm Theoretical Basis Document [RD 2]. Basic accuracy requirements are defined in the product requirements document [AD 2]. An extensive description of the instrument and satellite characteristics can be found in Hollinger (1987).

The CM SAF FCDR from SSM/I brightness temperatures is compiled as daily collections of all observations from each sensor. All sensor specific data available in the raw data records are provided as well as additional information like quality control flags, Earth incidence angles (EIA), averaged 85 GHz brightness temperatures, incidence angle normalisation offsets and intersensor calibration offsets. The FCDR is available for the time period from July 1987 until end of 2008. A detailed list of data availability for each of the six SSM/I platforms is given in Table 2-1.

3 Instrument and sensor stability

Figure 3-1 shows the time series of the mean DMSP platform local equator crossing times, altitude and the Earth Incidence Angles (EIA) of the different SSM/I instruments. The local overpass time is not constant for all platforms. The strongest drift can be observed for F14

Table 2-1: FCDR instrument data availability.

DMSP platform	Launch date	Record start	Record end
F08	1987-06-18	1987-07-09	1991-12-18
F10	1990-12-01	1991-01-07	1997-11-14
F11	1991-11-28	1992-01-01	1999-12-31
F13	1995-03-24	1995-05-03	2008-12-31
F14	1997-04-04	1997-05-07	2008-08-23
F15	1999-12-12	2000-02-28	2006-07-31

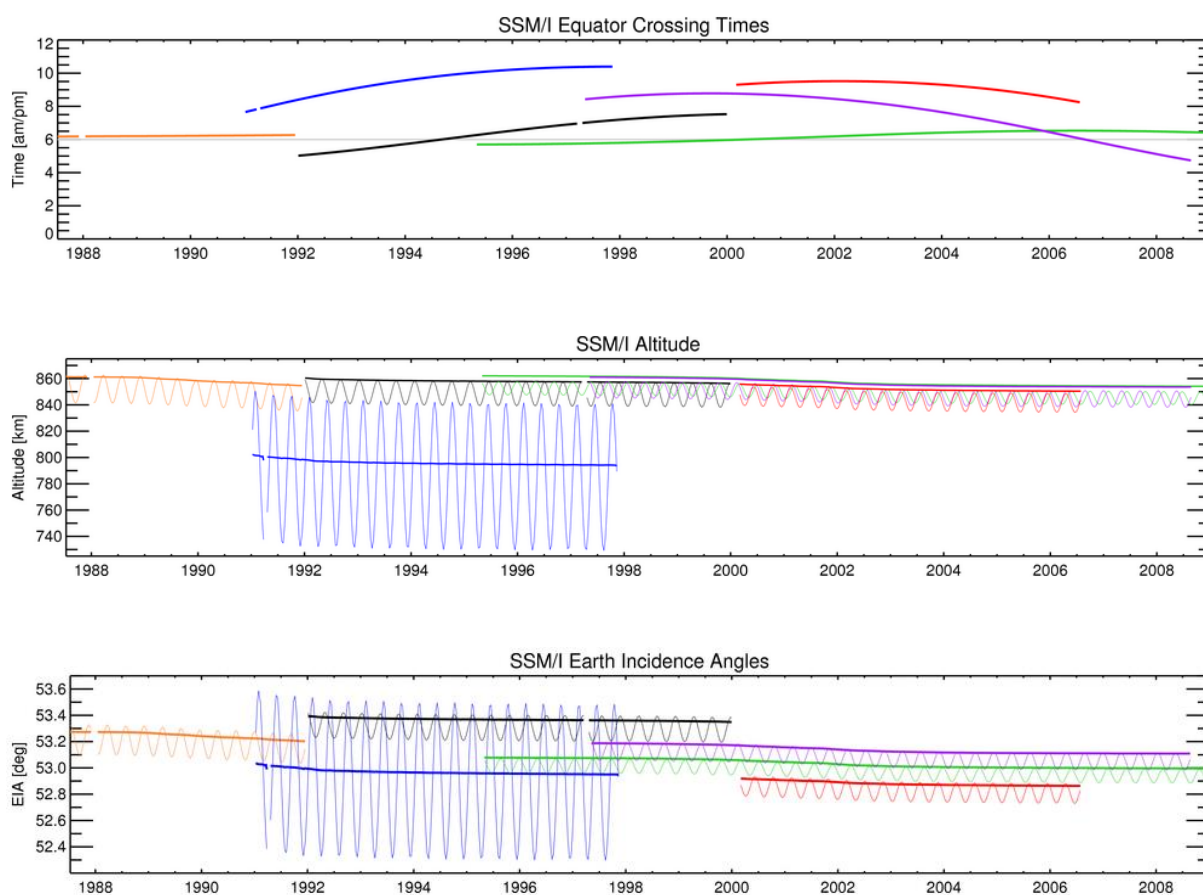


Figure 3-1: Time series of DMSP platform mean local equator crossing times, altitude and the Earth Incidence Angles of the different SSM/I instruments. Thin lines are the mean values at the ascending equator crossing and thick lines depict complete orbit mean values. Colours are as follows: F08 orange, F10 blue, F11 black, F13 green, F14 violet, and F15 red.

from 8 to 4 AM/PM while F13 and F08 show the most constant equator crossing time at 6 AM/PM. Due to the drift in overpass time, the brightness temperature (TB) differences between the instruments are not constant and the diurnal cycle variation must be taken into account when comparing the inter satellite differences.

Moreover, the altitude of the satellite platforms is not constant over time. As depicted in the centre panel of Figure 3-1, a small steady decrease of the altitude can be observed over the lifetime of all instrument platforms. This decrease in altitude leads to a decrease in EIA (Figure 3-1, lower panel). Particularly the EIA of F10 also exhibits a strong variation of about 1 degree with a period of 120 days due the highly elliptical orbit of the spacecraft. Since a change of 0.1 degree in EIA will change the vertical polarized TB up to 0.2 K, these variations must be taken into account by normalizing the observed TBs to a constant EIA.

CM SAF FCDR data files contain offsets, which are computed using the Furhop and Simmer (1996) algorithm to normalize the TBs to 53° EIA.

Figure 3-2 shows the time series of the hot load target temperatures for all instruments. The temperature of the warm calibration target exhibits a strong seasonal variability with an amplitude of up to 50 K for some of the instruments. This variation depends on the amount of time spent in the Earth shadow during an orbit and thus on the local equator overpass time.

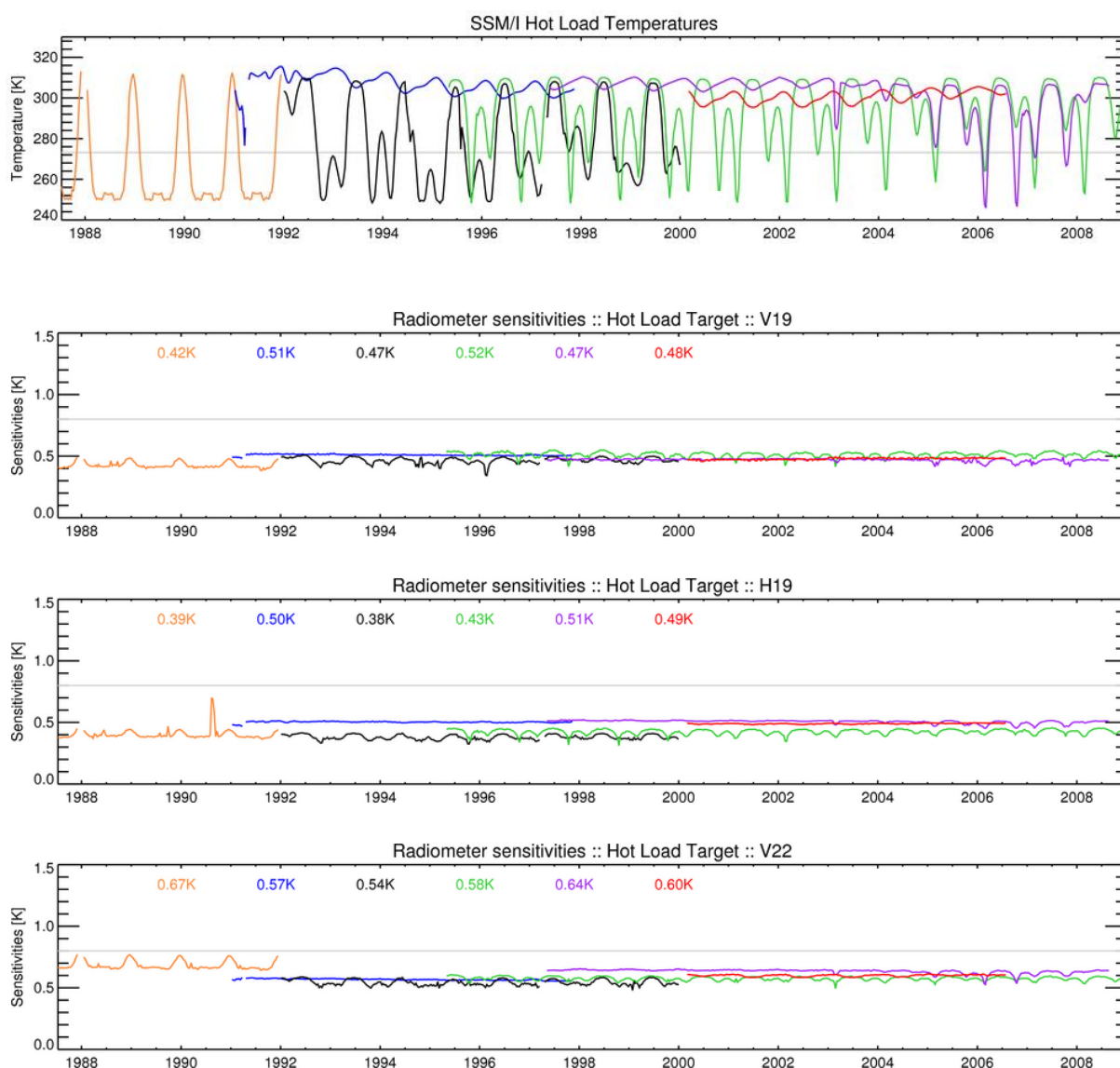


Figure 3-2: Time series of SSM/I sensor diagnostics: Temperature of the warm calibration target (upper panel) and radiometer sensitivities for the channels at 19v, 19h, and 22v GHz (centre and lower panel). The grey lines denote 0°C for the hot load temperature and the specification values for the radiometer sensitivities; for colours see Figure 3-1.

This can be seen for F14, which drifts from 8 AM/PM to 4 AM/PM. In the beginning the variation in warm target temperature is very small, but starts to undergo strong cooling events from 2005 onwards when the local overpass time has drifted before 7 AM/PM. The minima in the warm target temperatures are occurring at solar equinox in spring and autumn.

Figure 3-2 and Figure 4-1 also show the time series of the radiometer sensitivities for all SSM/I channels and sensors. This radiometer noise is estimated at the warm calibration target temperature and archived in the CM SAF FCDR data files. Overall, the radiometer noise is within the specification and constant for most of the channels, showing only a small variation due to the seasonal variation in warm target temperature. The most prominent feature is the known failure of the 85 GHz channels on-board F08 (see Figure 4-1). The vertical polarized channel noise strongly increases towards the end of 1987 until the instrument was switched off. The F08 85h channel noise steadily increases until early 1990 when it failed for the first time. It then recovers for a short period end of 1990 but finally failed shortly after that. Also the

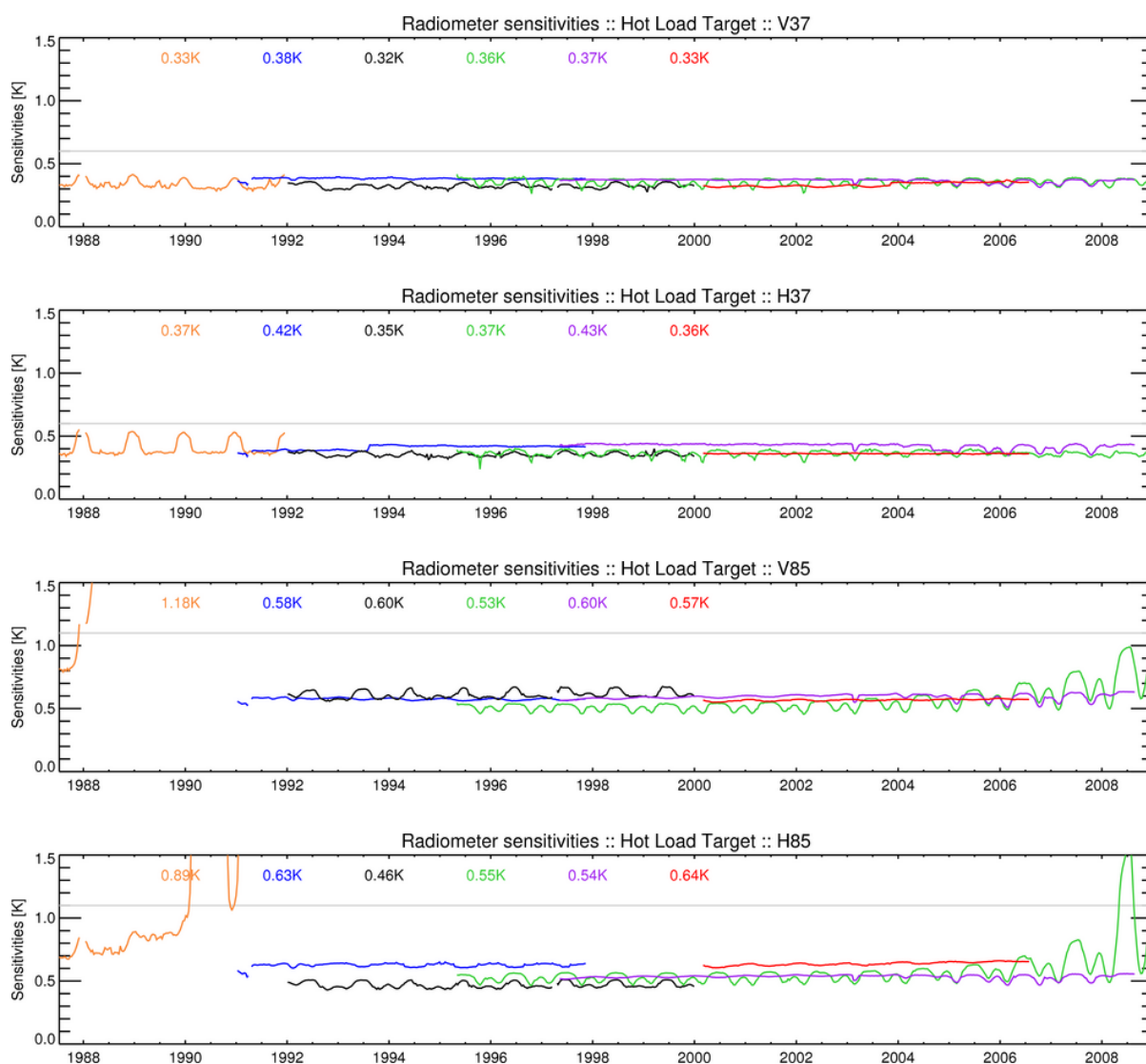



Figure 4-1: Time series of SSM/I sensor diagnostics: Radiometer sensitivities for the channels at 37v, 37h, 85v and 85h GHz. The grey lines denote the specification values; for colours see Figure 3-1.

85 GHz channels on-board F13 show a slow degradation over time with the seasonal amplitudes increasing year by year. The 85h channel finally exceeds the specification in 2008.

4 Evaluation of Brightness Temperature differences

The purpose of a validation is to establish that the measurement under scrutiny agrees with an independent, and (ideally) traceable, measurement or estimate, within the combined measurement uncertainties in both. A conclusion from the error budget estimation (see PUM [RD 1]) is that a complete comprehensive validation of the SSM/I brightness temperatures is not possible, as there is no absolute validation reference available. Hence, the final aim of an evaluation process must be to show that the measured SSM/I brightness temperatures are in agreement with modelled brightness temperatures within the expected random uncertainties. As a major requisite, a Fundamental Climate Data Record must show an improved quality compared to the existing Raw Data Records (RDR) in order to be a useful data set, providing an added value to the user community.

	Validation Report Microwave Imager Radiance FCDR R4 SSM/I Brightness Temperatures	Doc. No: SAF/CM/DWD/VAL/FCDR_SSM/I Issue: 1.2 Date: 2022-01-31
---	--	--

Hence, the validation strategy in this document is to compare this FCDR of SSM/I brightness temperatures to the original RDR and to the RSS Version-6 SSM/I FCDR (Semunegus, 2011), in order to quantify the quality of the inter-sensor calibration (see Product User Manual, [RD 1]) and to compare the different inter-sensor calibration approaches. The aim of this validation report is to show that the homogeneity of the reprocessed FCDR is significantly improved compared to the original raw Temperature Data Records.

4.1 Data Sets for Comparison

Another FCDR of SSM/I brightness temperatures available to date is released from Remote Sensing Systems. The inter-sensor calibration model used for this data set is described in detail in Semunegus (2011). The RSS inter-calibration model is defined as:

$$\Delta T_A = A(\phi) + B(\phi) \cdot \cos\left(\frac{2\pi}{t_{year}}\right) + C(t) + \alpha \cdot (\bar{T}_h - \langle \bar{T}_h \rangle) \pm D \quad \text{Equation 1}$$

with

$$\begin{aligned} \phi &= \text{orbit angle} \\ A(\phi) &= \text{intersatellite zonal offset} \\ B(\phi) &= \text{seasonal variation of intersatellite offset} \\ C(t) &= \text{slow time variation in the intersatellite offset} \\ \alpha \cdot (\bar{T}_h - \langle \bar{T}_h \rangle) &= \text{hot load target factor} \\ D &= \text{Diurnal variability} \end{aligned}$$

This model is more complicated and has more degrees of freedom than the CM SAF model. Similar to the CM SAF FCDR, it uses a relative inter-calibration but with the F13 as reference. The main correction coefficients $A(\phi)$ are found as zonal dependent offsets with 10 degrees separation. Additional to these constant offsets also time dependent coefficients $C(t)$ are used to correct for drifts in F10, F11, and F13. Mainly for F10 also a seasonal latitude dependent offset $B(\phi)$ is added, which corrects observed differences in the 85h channel. To account for the non-linear instrument response a hot load target factor α is used which relates the non-linearity effect to a linear deviation of the hot load target temperature \bar{T}_h from the mission mean temperature $\langle \bar{T}_h \rangle$. Finally, the EIA in the RSS FCDR is corrected with a slowly varying function of time. All together more than 260 fixed terms are found to minimize the observed differences to the reference instrument on F13.

4.2 Visual inspection

Before evaluating the TB differences statistically, a visual inspection of all satellite pairs has been done to test the performance of the intersensor calibration models over all surface types. The warmest TBs over land are not used directly during the model fitting procedure of the CM SAF FCDR due to the strong diurnal cycle of the land surface. However, the mean diurnal variability over land is the same for both polarizations. Thus double differencing can be used

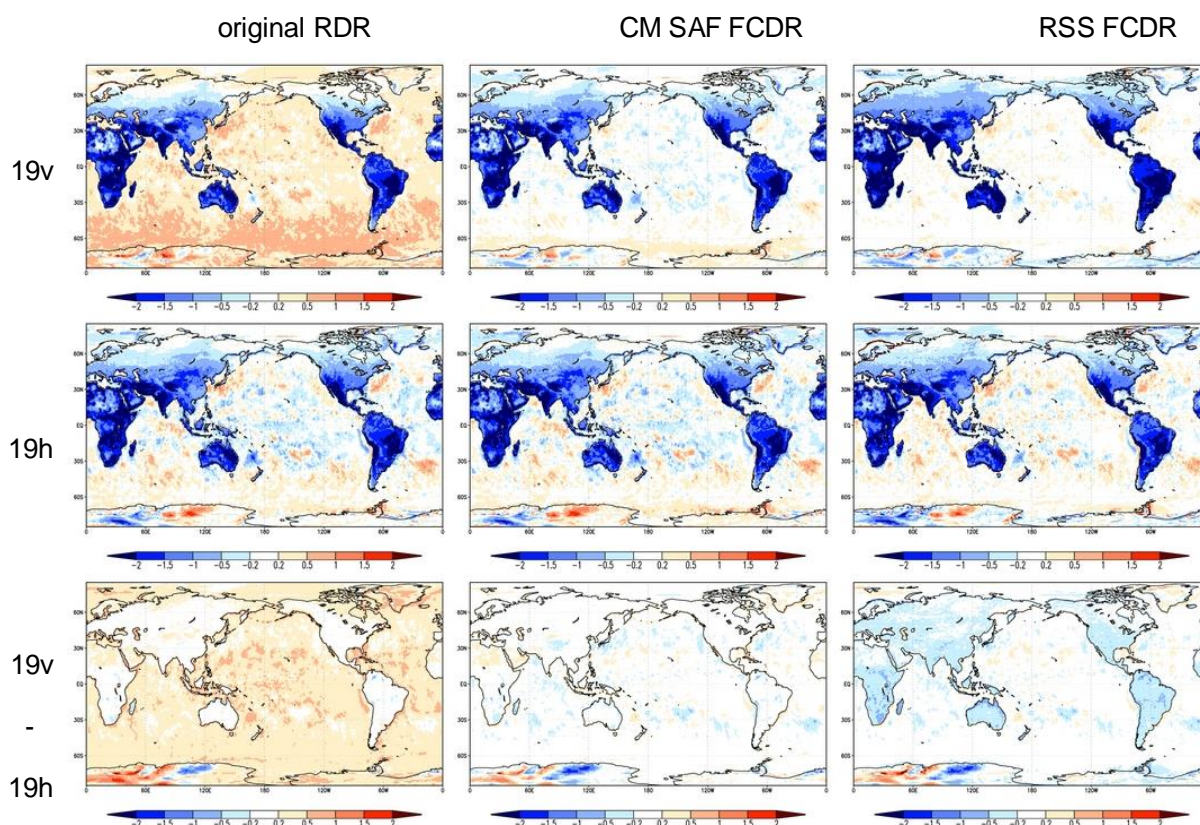


Figure 4-2: Climatological mean of SSM/I TB differences at 19 GHz between F13 and F15. In the left column shows the original uncorrected raw data records. The middle column depicts the CM SAF FCDR and the right column shows the RSS FCDR. The top row shows the vertical polarisation, the middle row the horizontal polarisation and in the bottom row depicts the double differences between both polarisations.

to remove the diurnal effects. As the result of these comparisons two examples are presented in Figure 4-2 and Figure 4-3. The figures show the climatological daily mean (AM and PM) of SSM/I TB differences at 19 GHz between F13 and F15 (Figure 4-2) and between F11 and F10 (Figure 4-3). The examples are chosen because between F13 and F15 the overpass time difference is large and between F10 and F11 the EIA difference is the maximum.

Both FCDRs remove the observed differences over the oceans. The remaining anomalies show nearly the same geographically distributed patterns. However, for the F13/F15 pair the RSS data show a remaining negative difference between 0.2 and 0.5 K over land areas. Also for the F11/F10 pair a negative bias (0.5-1 K) over land and arctic sea ice remains in the RSS FCDR. The CM SAF FCDR only shows a small positive bias over the Sahara desert. The large differences over Antarctica are caused by the gridding procedure and are artificial.

The other difference maps for channels and instrument pairs not presented here, show similar results but with larger noise at higher frequencies. The largest differences are found for the F10/F11 pair at 85 GHz over ocean. This is mainly caused by an approximation of the TB EIA dependence. The Furhop and Simmer (1996) method is not available for 85 GHz channels and a constant slope is used to correct for the EIA dependence.

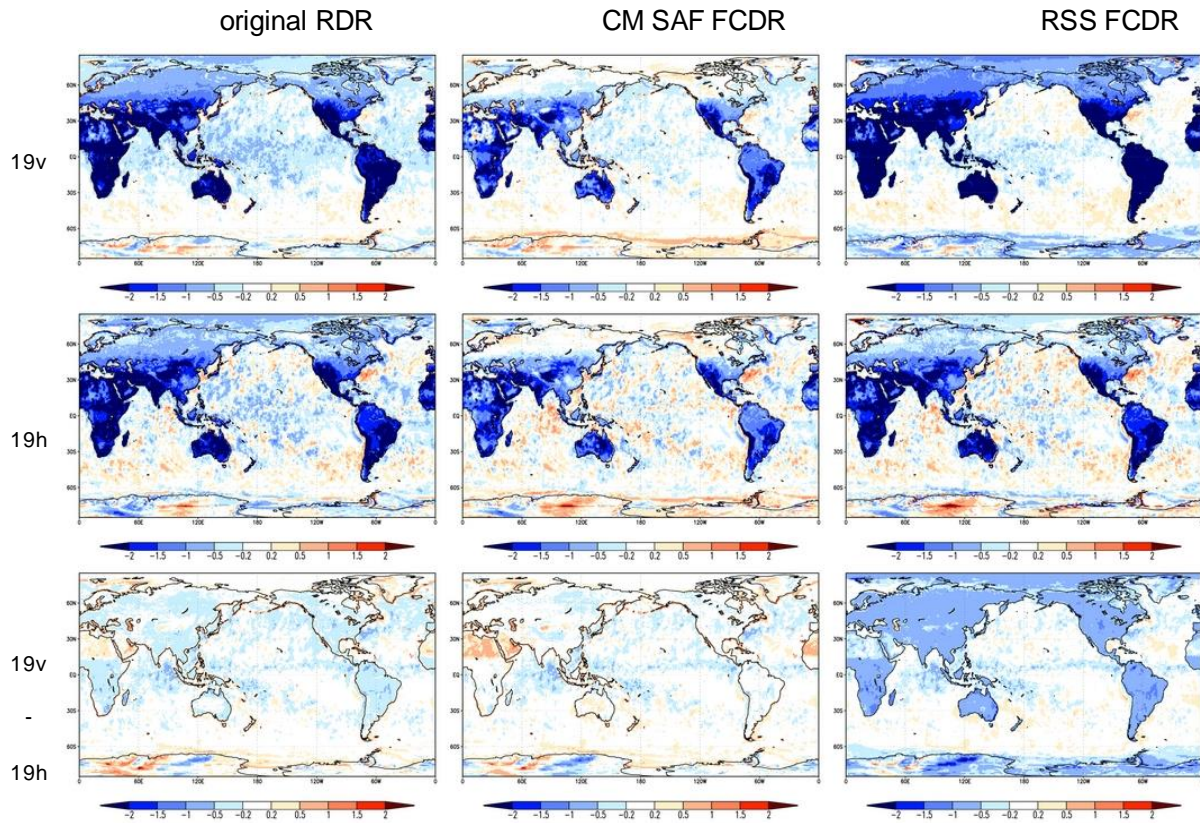


Figure 4-3: As Figure 4-2 but for the SSM/I TB differences at 19 GHz between F11 and F10.

4.3 Evaluation strategy

Similar to the visual inspection, the CM SAF FCDR is compared to the RDR and RSS brightness temperature data set. The homogeneity of the data sets is tested by comparing against the respective ensemble mean of the available satellites in each data record and additional statistical values are given for bias, RMS, and decadal stability.

The RSS data set used in this study covers the time period from July 1987 to end of 2006. The data files have first been converted to the CM SAF data format. Then both data sets have been gridded to equal angle 1° monthly mean global fields separately for AM and PM orbits. For the comparisons all oceanic and sea-ice covered grid cells are used plus land grid cells north and south of 65° latitude.

To evaluate the relative instrument differences an ensemble mean data set has been compiled for each FCDR on a monthly basis for all instruments and channels:

$$\langle T_B \rangle(t, g) = \frac{1}{n(t)} \cdot \sum_s T_B(s, t, g), \quad \text{Equation 2}$$

where t is the corresponding month, s is the instrument and g is the grid box index.

The differences relative to this ensemble mean

$$\Delta T_B(s, t, g) = T_B(s, t, g) - \langle T_B \rangle(t, g) \quad \text{Equation 3}$$

are statistically analyzed. The results are to be compared against the product requirement as summarized in Table 4-1.

The quantification of an RMS value for the TB differences is a difficult task because the main variability between the monthly mean TBs is due to the natural variability caused by the difference in overpass time and the sampling variability. However, it is possible to estimate the variability caused by systematic differences in the SSM/I calibration between the instruments. A systematic bias in the calibration can be assumed at first order as a function of the scene temperature. A global TB average will therefore contain a systematic offset $Bias_{sys}$ and a variability Var_{sys} caused by this systematic error. To estimate this variability the database of TB differences is binned and averaged at fixed percentiles p of the ensemble mean TB:

$$\Delta T_B(s, p) = \frac{1}{n} \sum_{t,g} \Delta T_B(s, t, g) \Big|_p \quad \text{Equation 4}$$

This averaging process thus removes the radiometric noise and minimizes the noise caused by the natural variability at a constant scene temperature. Then the averaged binned values can be used as new data set and $Bias_{sys}$, MAD_{sys} , and Var_{sys} are estimated from these percentile averages:

$$\begin{aligned} Bias_{sys}(s) &= \frac{1}{n} \sum_p \Delta T_B(s, p) \\ MAD_{sys}(s) &= \frac{1}{n} \sum_p |\Delta T_B(s, p)| \\ Var_{sys}(s) &= \frac{1}{n-1} \sum_p (\Delta T_B(s, p) - Bias_{sys}(s))^2 \\ SD_{sys}(s) &= \sqrt{Var_{sys}(s)} \end{aligned} \quad \text{Equation 5}$$

These values do not quantify the absolute systematic error but the relative error between the instruments and hence the consistency with the reference radiometer. Comparing the values before and after inter-calibration measures the goodness of the applied model, because an optimal inter-sensor calibration must minimize both, $Bias_{sys}$ and Var_{sys} .

To monitor the quality of the homogenization over time the global robust standard deviation RSD for each channel and instrument at time step t is computed as:

$$RSD(t) = med_g \left(\left| med_g(\Delta T_B(t, g)) - \Delta T_B(t, g) \right| \right) \cdot 1.48$$

The decadal stability td for each channel and instrument is estimated using a linear regression fitted to the anomalies of the instruments from the global mean values against the global ensemble mean:

Table 4-1: Requirements for SSM/I brightness temperatures product as given in the PRD [AD 2].

	Threshold	Target	Optimal
Bias	1.25 K	1.00 K	0.50 K
RMS	3.10 K	1.50 K	0.30 K
Decadal stability	0.20 K	0.08 K	0.03 K

$$\overline{\Delta T_B}(t) = \frac{1}{n} \cdot \sum_g (T_B(t, g) - \langle T_B \rangle(t, g))$$

$$\overline{\Delta T_B}(t) = t_D \cdot t + \overline{\Delta T_B}(t_0) + \varepsilon(t)$$

Equation 6

The results of the statistical analysis are shown in Figure 4-4 to Figure 4-10 and summarized in Table 4-2 to Table 4-8 grouped by channel. All figures contain 5 images with time series of monthly mean values of:


1. TB anomalies of the raw data record,
2. TB anomalies after EIA normalization and diurnal cycle removed,
3. TB anomalies of the CM SAF FCDR,
4. TB anomalies of the RSS FCDR,
5. Robust standard deviation (RSD) of CM SAF FCDR TB anomalies.

No trend estimates are computed for F08 because of the short overlap time period of only 12 months with F10.

4.4 Evaluation Results

The time series plots show that most of the TB differences are below 0.5 K before the inter-calibration but after applying the EIA normalization and removing the diurnal cycle. This proves the stable on-orbit calibration of the SSM/I instruments. Larger differences in the ensemble spread occur at the 85 GHz channels. Generally, the observed differences before applying the inter-calibration offsets are well within the estimated standard uncertainty of the SSM/I instrument, which is about 0.6 to 1 K (see ATBD [RD 2]).

- The largest monthly variability is found for the vertically polarized channels on-board F10 before EIA normalization, which is caused by the strong variation of the EIA, and underlines the importance of accounting for this either directly or by an EIA normalization.
- Overall, the monthly anomalies show a seasonal variability which is larger for horizontally polarized channels and increases with higher frequencies. This variability correlates with the warm target temperature variations and is significantly reduced by the inter-calibration model due to the inclusion of a non-linear coefficient. The RSS model contains a hot load target factor which also accounts for these variations but adds the same offset to all scene temperatures. Hence, it only corrects the mean values and does not depend on the scene temperature.
- Both FCDRs significantly reduce the observed differences between the monthly means and show very similar results. For some channels the CM SAF FCDR is performing slightly better, while for others the RSS FCDR. Comparing the offsets between the FCDRs reveals the largest differences for the vertically polarized channels and the 85h channel onboard F10. For these channels additional time dependent offsets are applied in the RSS model to remove these anomalies, leading to slightly lower ensemble

	Validation Report Microwave Imager Radiance FCDR R4 SSM/I Brightness Temperatures	Doc. No: SAF/CM/DWD/VAL/FCDR_SSMI Issue: 1.2 Date: 2022-01-31
---	--	---

anomalies compared to the CM SAF FCDR. However, it remains unclear, to what extend the differences are related to variability caused by the elliptical orbit of the F10.

- Moreover, the F10 shows an anomalous behaviour at the end of its lifetime in 1997. This can be attributed to a change in the spacecraft pitch and roll angles (Berg et. al, 2012). The observed difference of 0.2 K in the 19v channel can be explained by a change in 0.1° in EIA caused by a change in pitch angle. The CM SAF FCDR is computed using constant mission mean attitude corrections for each platform. Applying a variable pitch and roll correction could remove the observed increase in F10 TBs. However, since the uncertainty of the derived pitch correction translates to an uncertainty of about 0.1° in EIA (Berg et. al, 2012) these corrections must be carefully examined.
- The v22 channel on-board F15 is affected by a RADCAL beacon after August 2006. Although a correction is applied in the RSS data set a strong degradation is still visible in the comparison. Also the 85h channel is significantly affected as well as 19h and 37h to a lesser extent. F15 data should not be used for climatological applications and the CM FCDR does not contain F15 data after August 2006 (see Table 2-1).
- The robust standard deviations show nearly constant values over the time for all channel and satellites. The dominant feature is a larger variability of the F11 channels between 1995 and 1998. Also the F10/F08 period exhibits increased variability for early 1991. This is caused by a poor data availability of F10 in the beginning of 1991.
- Analysing the statistics derived from the data sets shows again a very good and similar performance of both data sets in terms of mean bias. The RSD of ensemble differences is consistently smaller in the CM SAF FCDR compared to RSS. The variability is about 5% smaller in the CM SAF FCDR. Also the estimated relative systematic variability is smaller in the CM SAF data set for most of the channels. The CM SAF inter-calibration model can significantly reduce the systematic variability by up to 70% as compared to the uncorrected data. This clearly proves existing scene dependent offsets, which are corrected by the inter-calibration model.
- The absolute differences between the CM SAF and RSS FCDR are within 0.5 K for most of the channels. The largest difference occurs at the 85v channel with 0.9 K. However, this is still within the expected absolute calibration uncertainty of the SSM/I.

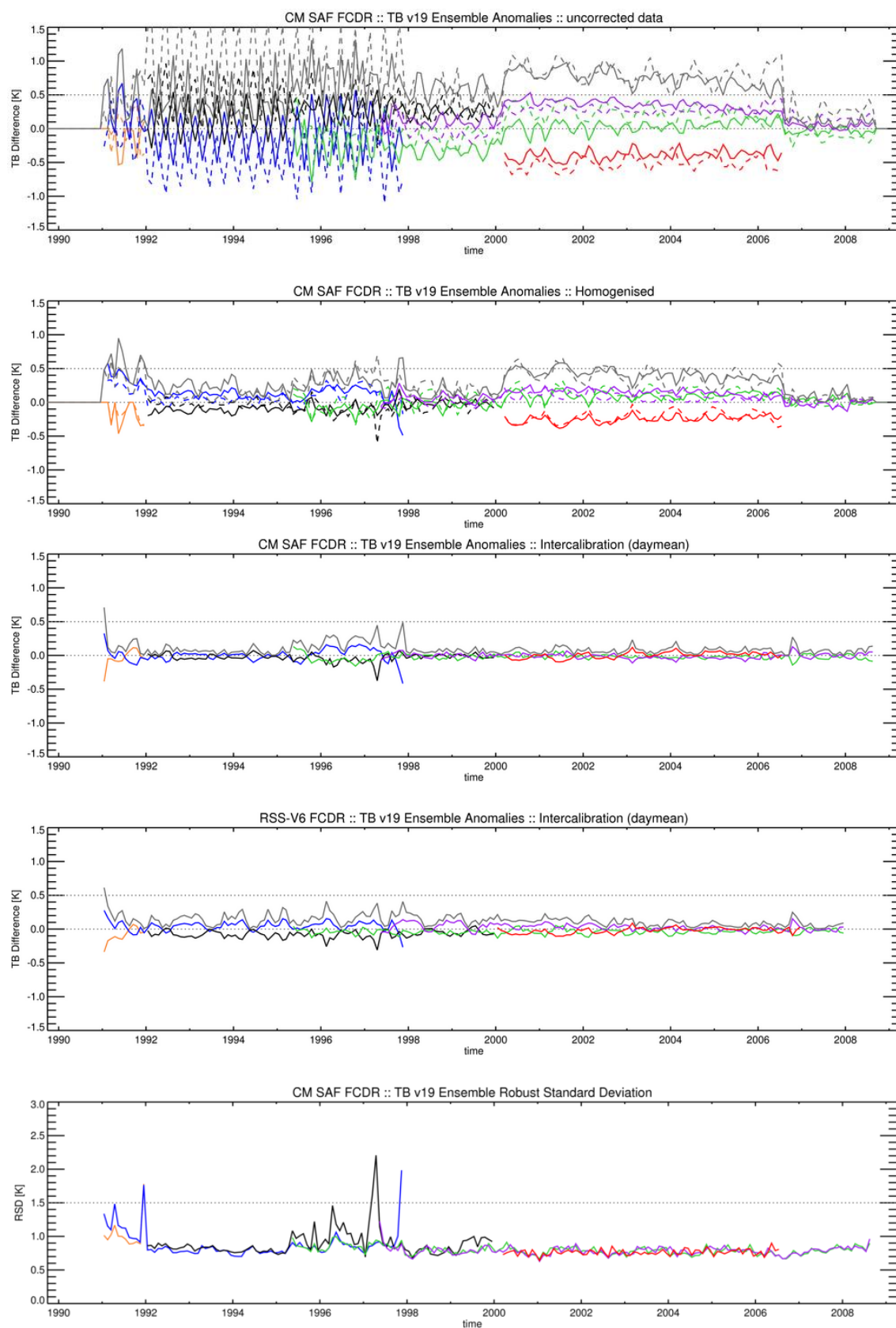


Figure 4-4: Time series of ensemble anomalies and variability for SSM/I channel 19v GHz. In the upper two panels the solid lines are PM orbits and the dashed lines AM orbits. The lower panels depict daily means of AM and PM orbits. The grey lines depict the ensemble spread. Horizontal dotted grey lines denote the optimal bias and the target RMS value (lowest panel). For a detailed description see text (section 4.3).


	Validation Report Microwave Imager Radiance FCDR R4 SSM/I Brightness Temperatures	Doc. No: SAF/CM/DWD/VAL/FCDR_SSMI Issue: 1.2 Date: 2022-01-31
---	--	---

Table 4-2: Statistics of the ensemble anomalies for SSM/I channel 19v GHz. The first block shows the original RDR with EIA normalized, the second block the CM SAF FCDR and the last block the RSS V6 FCDR. The offsets depict the differences between CM SAF and RSS over ocean.

	F08	F10	F11	F13	F14	F15
Bias_{sys} [K]	-0.31	0.12	-0.06	0.04	0.07	-0.24
SD_{sys} [K]	0.084 ±0.008	0.092 ±0.090	0.059 ±0.006	0.035 ±0.004	0.017 ±0.002	0.041 ±0.004
MAD_{sys} [K]	0.33	0.10	0.03	0.04	0.08	0.23
Bias_{sys} [K]	0.02	0.02	0.00	-0.01	0.00	0.01
SD_{sys} [K]	0.081 ±0.008	0.027 ±0.003	0.020 ±0.002	0.021 ±0.002	0.024 ±0.002	0.022 ±0.002
MAD_{sys} [K]	0.05	0.02	0.01	0.02	0.02	0.02
RSD_{ens} [K]	1.00	0.83	0.84	0.79	0.79	0.76
Trend [K/dec]		0.14 ±0.10	0.04 ±0.05	0.02 ±0.02	-0.02 ±0.02	0.11 ±0.05
Bias_{sys} [K]	-0.04	0.06	-0.04	-0.02	0.03	-0.02
SD_{sys} [K]	0.097 ±0.010	0.151 ±0.014	0.128 ±0.013	0.038 ±0.004	0.038 ±0.004	0.036 ±0.004
MAD_{sys} [K]	0.07	0.05	0.03	0.01	0.03	0.03
RSD_{ens} [K]	0.99	0.90	0.89	0.82	0.83	0.79
Trend [K/dec]		0.02 ±0.08	0.02 ±0.05	0.01 ±0.02	-0.09 ±0.07	0.13 ±0.04
Offset [K]	-0.48	-0.47	-0.49	-0.47	-0.45	-0.53

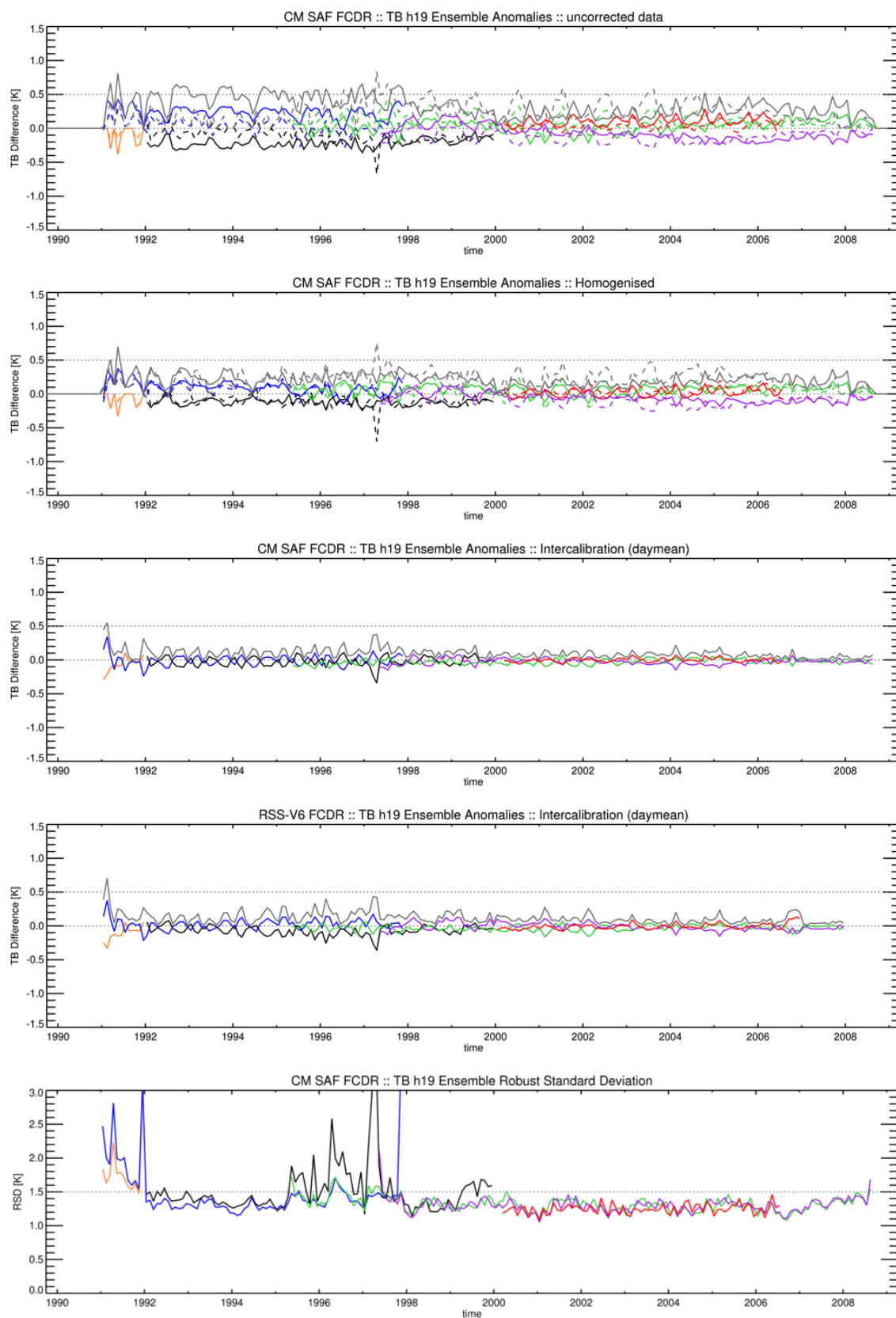


Figure 4-5: Same as Figure 4-4, but for SSM/I channel 19h GHz.

Table 4-3: Statistics of the ensemble anomalies for SSM/I channel 19h GHz. The first block shows the original RDR with EIA normalized, the second block the CM SAF FCDR and the last block the RSS V6 FCDR. The offsets depict the differences between CM SAF and RSS over ocean.

	F08	F10	F11	F13	F14	F15
Bias_{sys} [K]	-0.16	0.07	-0.08	0.07	-0.08	-0.04
SD_{sys} [K]	0.155 ±0.015	0.101 ±0.010	0.081 ±0.008	0.037 ±0.004	0.029 ±0.003	0.033 ±0.004
MAD_{sys} [K]	0.16	0.05	0.06	0.07	0.09	0.04
Bias_{sys} [K]	0.03	0.01	0.02	-0.02	0.00	0.01
SD_{sys} [K]	0.136 ±0.013	0.033 ±0.003	0.046 ±0.005	0.030 ±0.003	0.019 ±0.002	0.028 ±0.003
MAD_{sys} [K]	0.07	0.02	0.03	0.01	0.01	0.02
RSD_{ens} [K]	1.74	1.36	1.40	1.31	1.29	1.25
Trend [K/dec]		0.04 ±0.09	0.03 ±0.06	0.04 ±0.02	0.00 ±0.02	0.02 ±0.04
Bias_{sys} [K]	-0.01	0.02	-0.02	0.00	0.00	-0.01
SD_{sys} [K]	0.156 ±0.015	0.079 ±0.008	0.065 ±0.006	0.027 ±0.003	0.028 ±0.003	0.037 ±0.004
MAD_{sys} [K]	0.07	0.02	0.02	0.02	0.02	0.03
RSD_{ens} [K]	1.73	1.40	1.44	1.35	1.34	1.28
Trend [K/dec]		0.04 ±0.09	-0.01 ±0.06	0.03 ±0.02	-0.09 ±0.03	0.09 ±0.04
Offset [K]	-0.34	-0.21	-0.20	-0.11	-0.15	-0.18

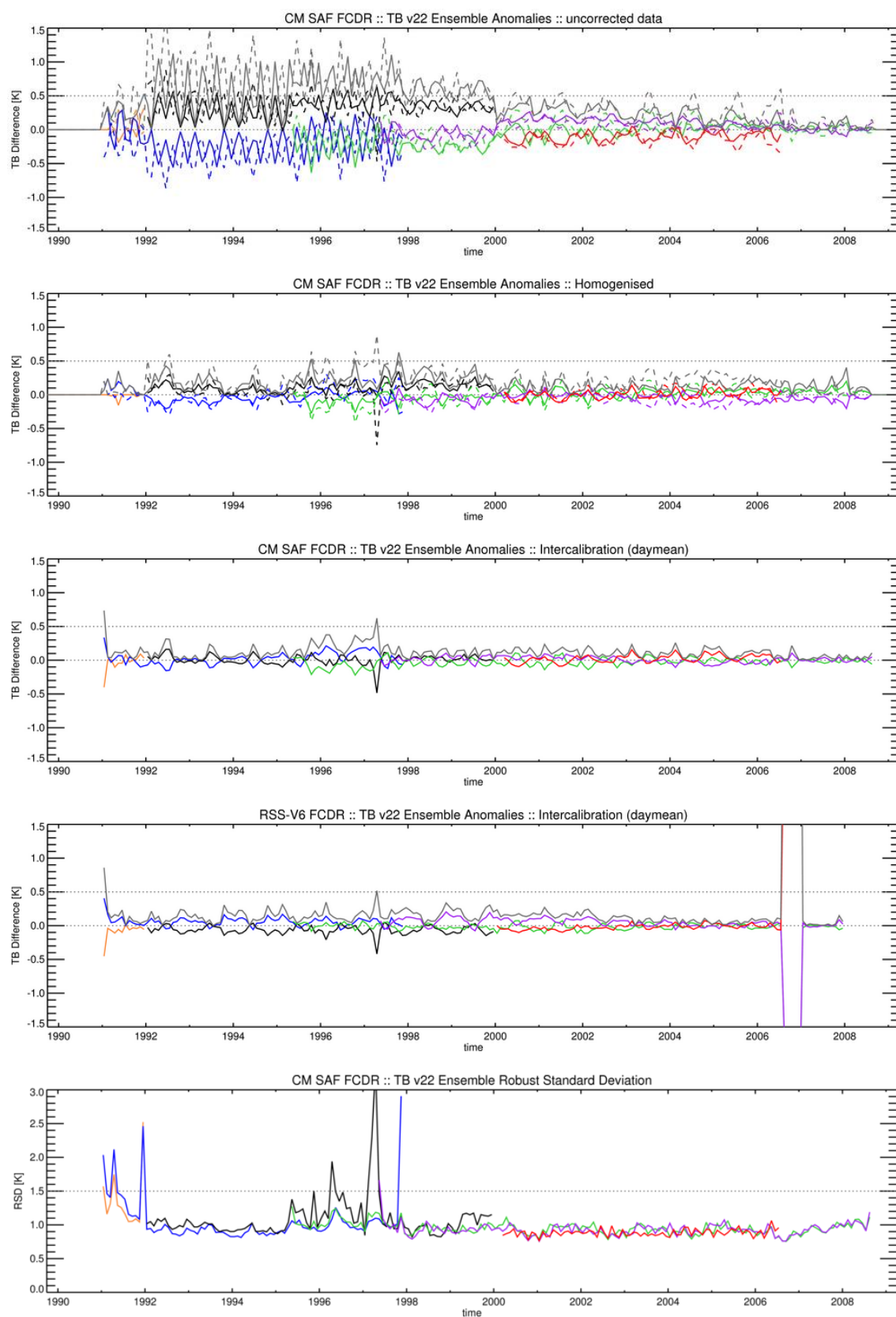


Figure 4-6: Same as Figure 4-4, but for SSM/I channel 22v GHz.

Table 4-4: Statistics of the ensemble anomalies for SSM/I channel 22v GHz. The first block shows the original RDR with EIA normalized, the second block the CM SAF FCDR and the last block the RSS V6 FCDR. The offsets depict the differences between CM SAF and RSS over ocean.

	F08	F10	F11	F13	F14	F15
Bias_{sys} [K]	-0.06	-0.01	0.10	-0.03	-0.04	0.03
SD_{sys} [K]	0.086 ±0.008	0.053 ±0.005	0.024 ±0.003	0.056 ±0.005	0.030 ±0.003	0.040 ±0.004
MAD_{sys} [K]	0.08	0.03	0.10	0.06	0.03	0.03
Bias_{sys} [K]	0.01	0.04	0.01	-0.05	0.02	0.02
SD_{sys} [K]	0.083 ±0.008	0.030 ±0.003	0.015 ±0.002	0.037 ±0.004	0.022 ±0.002	0.036 ±0.003
MAD_{sys} [K]	0.06	0.04	0.02	0.05	0.02	0.02
RSD_{ens} [K]	1.26	0.96	1.00	0.94	0.92	0.88
Trend [K/dec]		0.23 ±0.10	0.04 ±0.07	0.07 ±0.02	-0.04 ±0.02	0.11 ±0.06
Bias_{sys} [K]	-0.05	0.03	-0.03	-0.01	0.04	-0.03
SD_{sys} [K]	0.075 ±0.007	0.076 ±0.007	0.054 ±0.005	0.028 ±0.003	0.018 ±0.002	0.025 ±0.003
MAD_{sys} [K]	0.07	0.08	0.03	0.03	0.04	0.04
RSD_{ens} [K]	1.22	0.98	1.03	0.97	0.96	0.90
Trend [K/dec]		0.00 ±0.07	-0.04 ±0.06	-0.01 ±0.02	-0.10 ±0.03	0.09 ±0.03
Offset [K]	-0.37	-0.41	-0.39	-0.30	-0.35	-0.41

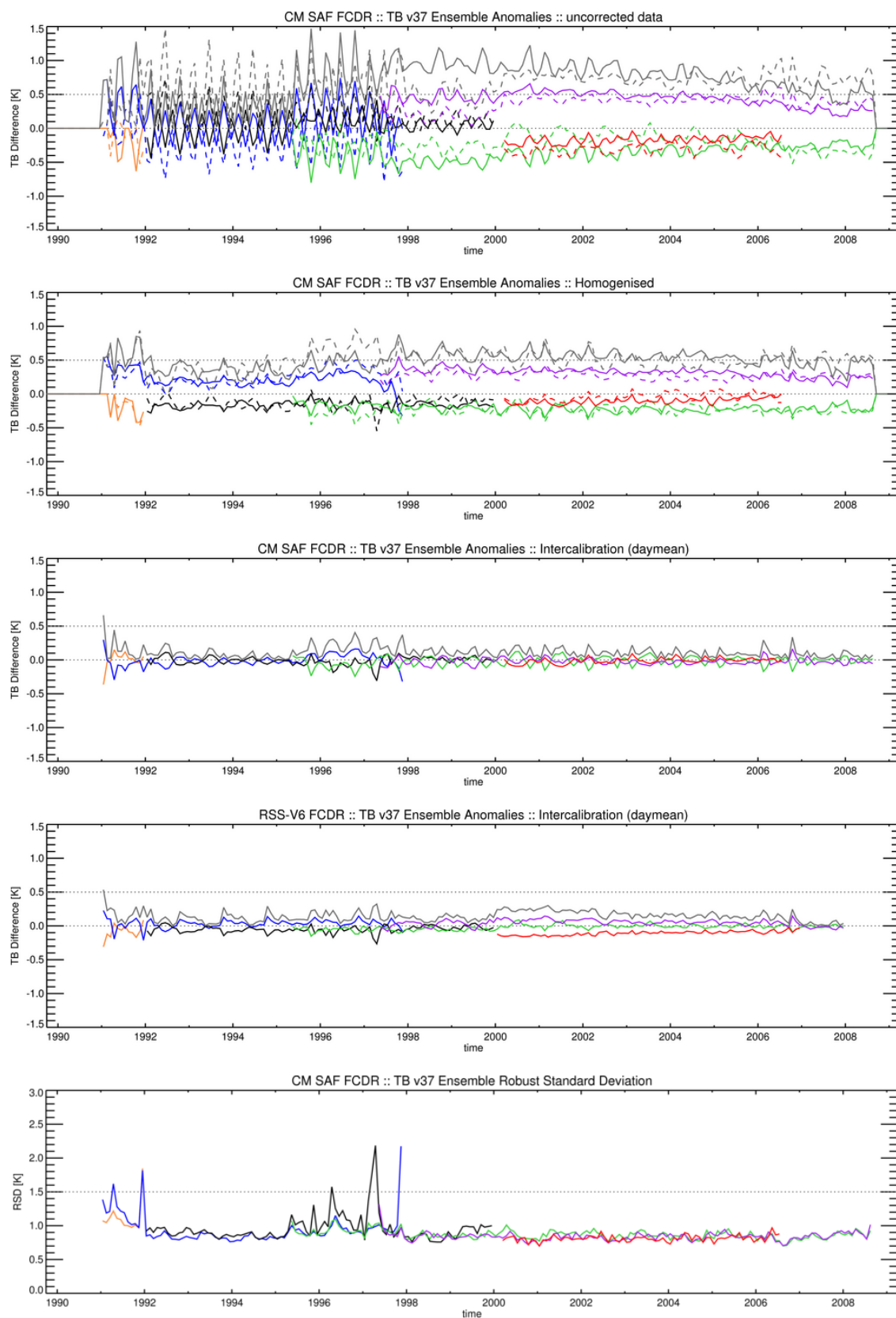


Figure 4-7: Same as Figure 4-4, but for SSM/I channel 37v GHz.

Table 4-5: Statistics of the ensemble anomalies for SSM/I channel 37v GHz. The first block shows the original RDR with EIA normalized, the second block the CM SAF FCDR and the last block the RSS V6 FCDR. The offsets depict the differences between CM SAF and RSS over ocean.

	F08	F10	F11	F13	F14	F15
Bias_{sys} [K]	-0.40	0.25	-0.16	-0.25	0.31	-0.05
SD_{sys} [K]	0.150 ±0.015	0.077 ±0.007	0.035 ±0.003	0.030 ±0.003	0.017 ±0.002	0.039 ±0.004
MAD_{sys} [K]	0.41	0.25	0.15	0.25	0.31	0.04
Bias_{sys} [K]	0.02	0.02	0.01	-0.02	0.00	0.01
SD_{sys} [K]	0.141 ±0.014	0.076 ±0.007	0.035 ±0.003	0.031 ±0.003	0.017 ±0.002	0.032 ±0.003
MAD_{sys} [K]	0.04	0.06	0.03	0.03	0.01	0.03
RSD_{ens} [K]	1.10	0.90	0.90	0.87	0.84	0.82
Trend [K/dec]		0.15 ±0.10	0.05 ±0.06	0.05 ±0.03	-0.02 ±0.03	0.10 ±0.05
Bias_{sys} [K]	-0.08	0.05	-0.02	-0.01	0.06	-0.08
SD_{sys} [K]	0.168 ±0.017	0.116 ±0.011	0.073 ±0.007	0.018 ±0.002	0.030 ±0.003	0.044 ±0.004
MAD_{sys} [K]	0.07	0.04	0.03	0.01	0.05	0.07
RSD_{ens} [K]	1.06	0.93	0.95	0.89	0.87	0.85
Trend [K/dec]		0.01 ±0.07	0.05 ±0.04	0.04 ±0.02	-0.02 ±0.03	0.14 ±0.02
Offset [K]	-0.39	-0.23	-0.21	-0.21	-0.20	-0.37

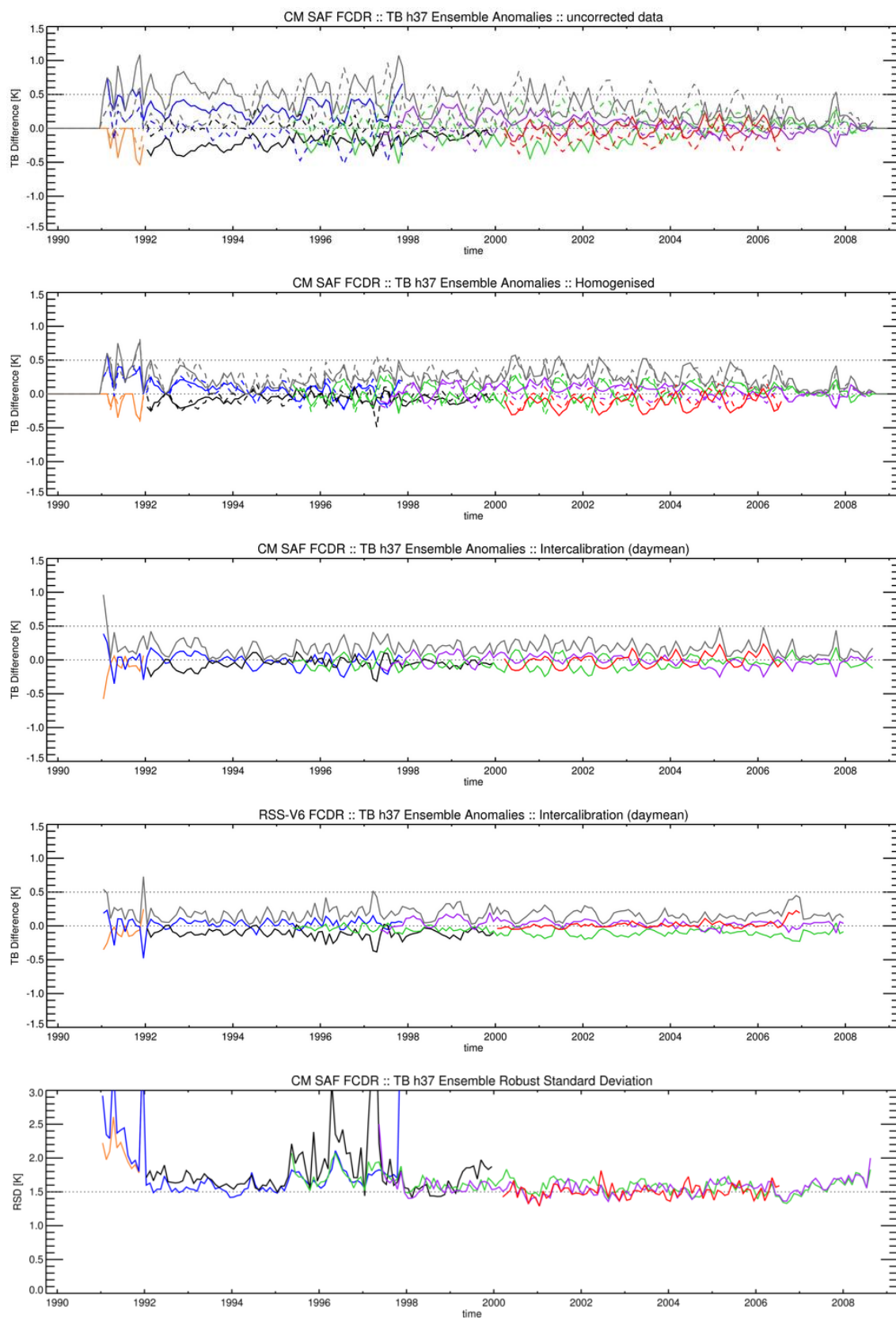


Figure 4-8: Same as Figure 4-4, but for SSM/I channel 37h GHz.

Table 4-6: Statistics of the ensemble anomalies for SSM/I channel 37h GHz. The first block shows the original RDR with EIA normalized, the second block the CM SAF FCDR and the last block the RSS V6 FCDR. The offsets depict the differences between CM SAF and RSS over ocean.

	F08	F10	F11	F13	F14	F15
Bias_{sys} [K]	-0.33	0.05	-0.01	0.04	0.01	-0.11
SD_{sys} [K]	0.210 ±0.020	0.091 ±0.009	0.087 ±0.008	0.062 ±0.006	0.061 ±0.006	0.052 ±0.005
MAD_{sys} [K]	0.29	0.02	0.03	0.07	0.03	0.13
Bias_{sys} [K]	-0.05	0.00	0.02	-0.02	0.01	0.00
SD_{sys} [K]	0.189 ±0.018	0.070 ±0.007	0.072 ±0.007	0.025 ±0.002	0.023 ±0.002	0.034 ±0.004
MAD_{sys} [K]	0.06	0.04	0.06	0.02	0.02	0.02
RSD_{ens} [K]	2.11	1.64	1.68	1.60	1.55	1.50
Trend [K/dec]		-0.16 ±0.12	0.07 ±0.07	0.02 ±0.04	-0.05 ±0.04	0.17 ±0.10
Bias_{sys} [K]	-0.04	0.03	-0.04	-0.03	0.03	0.01
SD_{sys} [K]	0.214 ±0.020	0.079 ±0.008	0.074 ±0.007	0.071 ±0.007	0.070 ±0.007	0.052 ±0.005
MAD_{sys} [K]	0.07	0.02	0.03	0.01	0.01	0.02
RSD_{ens} [K]	2.04	1.67	1.74	1.64	1.60	1.53
Trend [K/dec]		0.02 ±0.10	-0.03 ±0.06	0.08 ±0.02	-0.04 ±0.03	0.09 ±0.05
Offset [K]	0.04	0.03	-0.12	-0.06	-0.09	-0.10

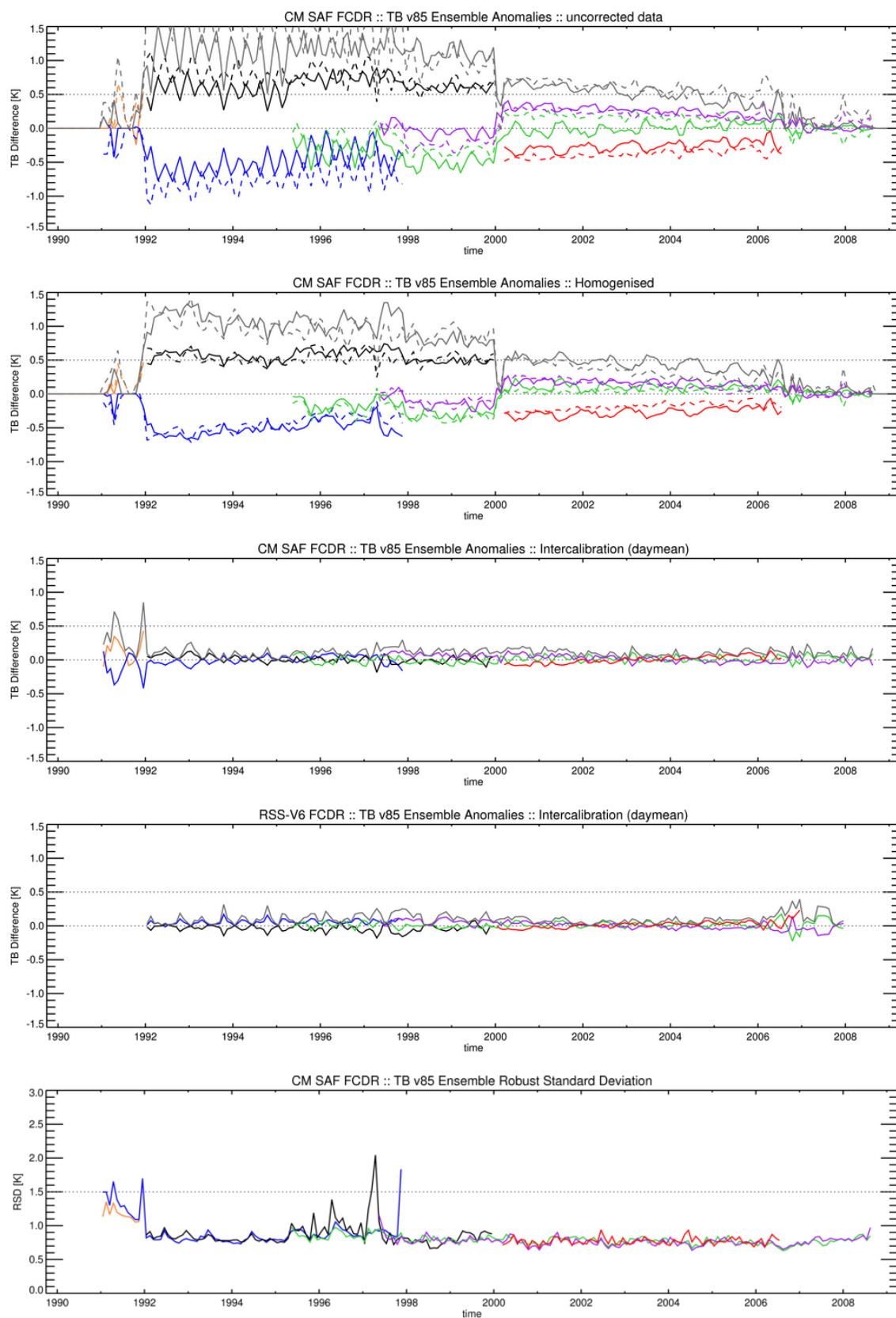


Figure 4-9: Same as Figure 4-4, but for SSM/I channel 85v GHz.


	Validation Report Microwave Imager Radiance FCDR R4 SSM/I Brightness Temperatures	Doc. No: SAF/CM/DWD/VAL/FCDR_SSMI Issue: 1.2 Date: 2022-01-31
---	--	---

Table 4-7: Statistics of the ensemble anomalies for SSM/I channel 85v GHz. The first block shows the original RDR with EIA normalized, the second block the CM SAF FCDR and the last block the RSS V6 FCDR. The offsets depict the differences between CM SAF and RSS over ocean.

	F08	F10	F11	F13	F14	F15
Bias_{sys} [K]		-0.49	0.56	-0.05	0.06	-0.23
SD_{sys} [K]		0.077 ±0.007	0.064 ±0.006	0.066 ±0.006	0.041 ±0.004	0.046 ±0.004
MAD_{sys} [K]		0.52	0.06	0.07	0.07	0.25
Bias_{sys} [K]		-0.02	0.00	0.00	0.01	-0.01
SD_{sys} [K]		0.077 ±0.007	0.072 ±0.007	0.021 ±0.002	0.020 ±0.002	0.034 ±0.003
MAD_{sys} [K]		0.06	0.05	0.02	0.02	0.03
RSD_{ens} [K]		0.83	0.81	0.79	0.77	0.77
Trend [K/dec]		0.17 ±0.08	-0.10 ±0.04	0.04 ±0.02	-0.13 ±0.02	0.28 ±0.04
Bias_{sys} [K]		0.05	-0.05	0.00	0.00	0.00
SD_{sys} [K]		0.103 ±0.010	0.107 ±0.010	0.023 ±0.002	0.012 ±0.001	0.052 ±0.005
MAD_{sys} [K]		0.04	0.04	0.02	0.01	0.04
RSD_{ens} [K]		0.85	0.86	0.79	0.77	0.76
Trend [K/dec]		0.07 ±0.05	-0.05 ±0.04	0.00 ±0.02	-0.15 ±0.02	0.18 ±0.04
Offset [K]		-0.89	-0.93	-0.89	-0.92	-0.91

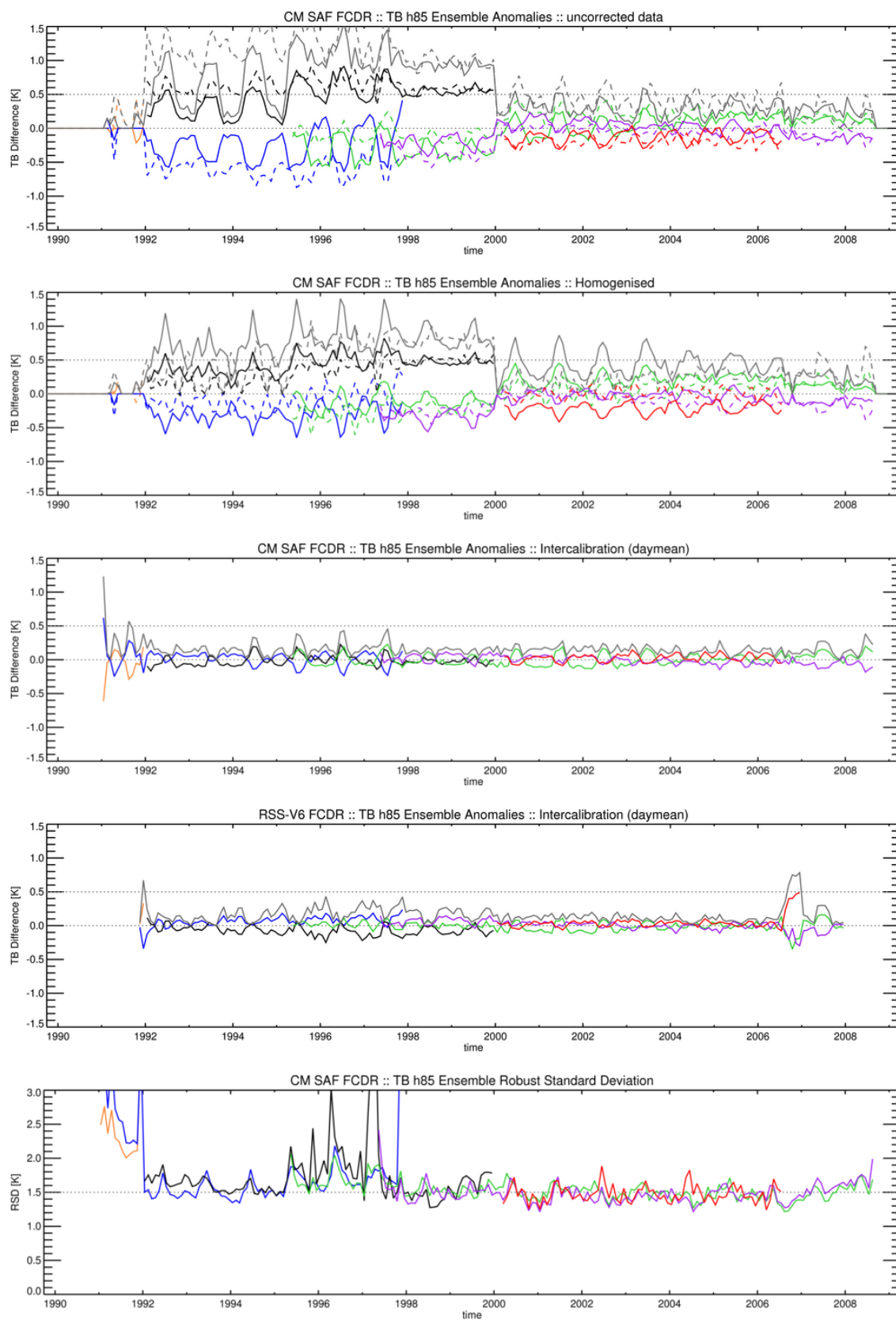


Figure 4-10: Same as Figure 4-4, but for SSM/I channel 85h GHz.



	Validation Report Microwave Imager Radiance FCDR R4 SSM/I Brightness Temperatures	Doc. No: SAF/CM/DWD/VAL/FCDR_SSM/I Issue: 1.2 Date: 2022-01-31
---	--	--

Table 4-8: Statistics of the ensemble anomalies for SSM/I channel 85h GHz. The first block shows the original RDR with EIA normalized, the second block the CM SAF FCDR and the last block the RSS V6 FCDR. The offsets depict the differences between CM SAF and RSS over ocean.

	F08	F10	F11	F13	F14	F15
Bias_{sys} [K]		-0.23	0.42	0.01	-0.11	-0.11
SD_{sys} [K]		0.109 ±0.010	0.108 ±0.010	0.068 ±0.007	0.060 ±0.006	0.054 ±0.006
MAD_{sys} [K]		0.25	0.44	0.07	0.11	0.13
Bias_{sys} [K]		-0.01	0.01	0.00	-0.01	0.01
SD_{sys} [K]		0.099 ±0.010	0.075 ±0.008	0.029 ±0.003	0.032 ±0.003	0.054 ±0.005
MAD_{sys} [K]		0.06	0.05	0.02	0.03	0.04
RSD_{ens} [K]		1.57	1.63	1.53	1.47	1.45
Trend [K/dec]		-0.12 ±0.12	0.08 ±0.07	0.09 ±0.04	-0.14 ±0.03	0.02 ±0.07
Bias_{sys} [K]		0.03	-0.04	-0.01	0.01	0.01
SD_{sys} [K]		0.086 ±0.008	0.088 ±0.008	0.036 ±0.003	0.043 ±0.004	0.066 ±0.006
MAD_{sys} [K]		0.04	0.05	0.02	0.04	0.05
RSD_{ens} [K]		1.61	1.67	1.55	1.51	1.48
Trend [K/dec]		0.20 ±0.08	-0.12 ±0.06	-0.03 ±0.03	-0.16 ±0.03	0.03 ±0.10
Offset [K]		-0.69	-0.67	-0.62	-0.63	-0.72

	Validation Report Microwave Imager Radiance FCDR R4 SSM/I Brightness Temperatures	Doc. No: SAF/CM/DWD/VAL/FCDR_SSM/I Issue: 1.2 Date: 2022-01-31
---	--	--

5 Conclusions

The CM SAF FCDR of SSM/I brightness temperatures has been evaluated to analyse the data set homogeneity and consistency and the goodness of the developed inter-calibration model. It was shown that the inter-calibration model works well over all surface types. The overall mean differences between the different sensors has been reduced to below 0.1 K. The observed seasonal variability has been significantly reduced with maximum remaining differences to the ensemble mean of about 0.25 K, depending on frequency and polarisation. This fulfils the optimum target accuracy for the bias. It should be noted that the CM SAF intercalibration model achieves the same or even better accuracies with a self-consistent inter-sensor calibration model that uses much less parameters compared to the RSS model.

The observed variability is mainly caused by the natural variability due to overpass time differences and sampling differences. However, the mean RMS for most of the channels and instruments is lower than 1 K and within the target accuracy and for channels at 37h and 85h lower than 2 K and thus within threshold accuracy. The relative systematic variability caused by different systematic calibration errors has been estimated from the data set. This variability has been significantly reduced by the inter-calibration model, proving that a scene dependent bias correction is performing better than a constant offset. This relative systematic error is between 0.02 K and 0.1 K for most of the instruments and channels.

The estimated decadal trends are mostly within optimum and target accuracy. Only the 85v channel on-board F15 shows a significant trend above threshold. The RSS FCDR is showing similar trends for most of the sensors. An exception are the F10 vertically polarized channels, which do not show a trend in the RSS data set because it has been explicitly removed by the RSS inter-calibration model. The observed trends can be partly explained by time varying changes in spacecraft attitude corrections (Berg et. al, 2012).

Finally it can be concluded that this FCDR is providing a greatly improved quality of the SSM/I brightness temperatures as compared to original raw data records.

6 References

Andersson, A., Fennig, K., Klepp, C., Bakan, S., Graßl, H., and Schulz, J.: The Hamburg Ocean Atmosphere Parameters and Fluxes from Satellite Data – HOAPS-3, *Earth Syst. Sci. Data*, 2, 215-234, doi:10.5194/essd-2-215-2010, 2010.

Andersson, A., C. Klepp, K. Fennig, S. Bakan, H. Graßl, and J. Schulz: Evaluation of HOAPS-3 ocean surface freshwater flux components, *Journal of Applied Meteorology and Climatology*, 50, 379-398, doi:10.1175/2010JAMC2341.1, 2011

Berg, W., Sapiano, M. R. P. ; Horsman, J. ; Kummerow, C., 2012: Improved Geolocation and Earth Incidence Angle Information for a Fundamental Climate Data Record of the SSM/I Sensors, *IEEE Transactions on Geoscience and Remote Sensing*, Early online release, doi: 10.1109/TGRS.2012.2199761

Fennig, K., Schröder, M., Andersson, A., and Hollmann, R.: A Fundamental Climate Data Record of SMMR, SSM/I, and SSMIS brightness temperatures, *Earth Syst. Sci. Data*, 12, 647–681, <https://doi.org/10.5194/essd-12-647-2020>, 2020.

Furhop, R. and Simmer, C.: SSM/I Brightness Temperature Corrections for Incidence Angle Variations, *J. Atmos. Oceanic Technol.*, 13, 246–254, 1996.


Hollinger, J., Poe, G..A.: Special Sensor Microwave/Imager User's Guide, Naval Research Laboratory Report, Washington DC, 1987

Poli, P.; Peubey C., Fennig K., Schröder M., Roebelling R., Geer A. (2015): Pre-assimilation feedback on a Fundamental Climate Data Record of brightness temperatures from Special Sensor Microwave Imagers: A step towards MIPs4Obs?, *ERA Report Series*, 19.


Semunegus, H: Remote Sensing Systems Version-6 Special Sensor Microwave/Imager Fundamental Climate Data Record, Climate Algorithm Theoretical Basis Document, Climate Data Record (CDR) Program, CDRP-ATBD-0100, 2011

7 Glossary

APC	Antenna Pattern Correction
ATBD	Algorithm Theoretical Baseline Document
CM SAF	Satellite Application Facility on Climate Monitoring
DMSP	Defense Meteorological Satellite Program
DWD	Deutscher Wetterdienst (German MetService)
ECI	Earth-centred inertial
ECMWF	European Centre for Medium Range Forecast
ECV	Essential Climate Variable
EIA	Earth Incidence Angle

	Validation Report Microwave Imager Radiance FCDR R4 SSM/I Brightness Temperatures	Doc. No: SAF/CM/DWD/VAL/FCDR_SSMI Issue: 1.2 Date: 2022-01-31
---	--	---

EPS	European Polar System
EUMETSAT	European Organisation for the Exploitation of Meteorological Satellites
FCDR	Fundamental Climate Data Record
FMI	Finnish Meteorological Institute
FOV	Field of view
GCOS	Global Climate Observing System
GLOBE	The Global Land One-kilometer Base Elevation
HOAPS	The Hamburg Ocean Atmosphere Fluxes and Parameters from Satellite data
IOP	Initial Operations Phase
KNMI	Koninkrijk Nederlands Meteorologisch Instituut
MD5	Message-Digest Algorithm 5
MSG	Meteosat Second Generation
NASA	National Aeronautics and Space Administration
NCEP	National Centers for Environmental Prediction
NDBC	National Data Buoy Center
NESDIS	National Environmental Satellite, Data, and Information System
NMHS	National Meteorological and Hydrological Services
NOAA	National Oceanic & Atmospheric Administration
NWP	Numerical Weather Prediction
PRD	Product Requirement Document
PUM	Product User Manual
QC	Quality Control
RMIB	Royal Meteorological Institute of Belgium
RMS	Root Mean Square
RSS	Remote Sensing Systems
SAF	Satellite Application Facility
SI	Système international d'unités
SMHI	Swedish Meteorological and Hydrological Institute

	Validation Report Microwave Imager Radiance FCDR R4 SSM/I Brightness Temperatures	Doc. No: SAF/CM/DWD/VAL/FCDR_SSMI Issue: 1.2 Date: 2022-01-31
---	--	---

SSM/I Special Sensor Microwave Imager

SSMIS Special Sensor Microwave Imager Sounder

TA Antenna Temperature

TB Brightness Temperature

TDR Temperature Data Records